⊙ 研究論文

A Study on Flow Characteristics of Two-Dimensional Backward-Facing Step by CFD

Y. D. Choi · Y. H. Lee

CFD에 의한 2차원 후향계단에서의 재부착 유동특성에 관한 연구

최 영 도* · 이 영 호**

Key words : Backward-facing step, Navier-Stokes equation, Reynolds number, Reattachment length, irregular staggered grid

Abstract

The present study is aimed to investigate flow characteristics of two-dimensional backward-facing step by numerical approach. A convection conservative difference scheme based upon SOLA algorithm is used for the solution of the two-dimensional incompressible Navier-Stokes equations to simulate the laminar, transitional and turbulent flow conditions at which the experimental data can be available for the backward-facing step. The twenty kinds of Reynolds number are used for the calculations. In an effort to demonstrate that the reported solutions are dependent on the mesh refinement, computations are performed on seven different meshes of uniformly increasing refinement. Also to investigate the result of inflow dependence, two kinds of the inflow profile are chosen for the laminar flow. Irregular grid system is adopted to minimize the errors on the satisfaction of the discretized continuity. As criterion of benchmarking, the result of numerical simulation, reattachment length is used for the selected Reynolds numbers. The results of the present study prove the fact that the numerical predictions agree well with the experimental data and the flow characteristics are shown at the backward-facing step.

1. INTRODUCTION

The laminar or the turbulent flow over a backward - facing step is one of the simplest but very important separate flows which is frequently used as a benchmark problem to test

* Regular member, Daewoo Heavy Industries Ltd.(receipt : '98. 3.)
** Regular member, Korea Maritime University, School. of Mechanical Eng.

the computational fluid dynamics method.

The importance of such a flow can be found in engineering equipment in which sudden expansions of section geometries cause the flow separation and reattachment.

A number of experimental and numerical studies have been made for this problem to investigate the phenomena of separation and reattachment of shear flows including the variation of flow structure with Reynolds number, the section geometry or the step height, and the momentum thickness of the oncoming flow to the step. The experimental and computational investigation of Armaly et al.[1] could be the most directly related and widely known works published. The thorough review and analysis of experimental data by Eaton and Johnston[2] and the experimental study of Kim et al.[3] could be representative works in the literature. The workshop[4] held by KSME showed various results as per the numerical algorithms used.

The purpose of the present works is to carry out a numerical investigation into separating laminar, transitional and turbulent flows over a backward-facing step using a convection conservative difference scheme based upon SOLA algorithm for the solution of the two-dimensional incompressible Navier-Stokes equations.

Comparisons are made with the measurements of Armaly et al. to aid in evaluating the present numerical method.

2. NUMERICAL METHOD

Navier-Stokes equations are governing equations in the form of partial differential equation, which describe the motion of fluid particles around a point of continuum flow. In the Cartesian coordinates(x,y), with x measured from the step and y normal to the bottom wall, the equations governing the incompressible, unsteady, viscous, two-dimensional flow can be written in the conservation form with dimensionless variables as:

$$\frac{\partial u}{\partial x}+\frac{\partial v}{\partial y}=0 \tag{1}$$

$$\frac{\partial u}{\partial t}+\frac{\partial u\cdot v}{\partial x}+\frac{\partial v\cdot u}{\partial y}=-\frac{\partial p}{\partial x}+g_x+\frac{1}{Re}\left(\frac{\partial^2 u}{\partial x^2}+\frac{\partial^2 u}{\partial y^2}\right) \tag{2}$$

$$\frac{\partial v}{\partial t}+\frac{\partial u\cdot v}{\partial x}+\frac{\partial v\cdot v}{\partial y}=-\frac{\partial p}{\partial y}+g_y+\frac{1}{Re}\left(\frac{\partial^2 v}{\partial x^2}+\frac{\partial^2 v}{\partial y^2}\right) \tag{3}$$

where (u,v) and (g_x, g_y) are, respectively, the velocity and gravitational acceleration components in the (x,y) directions, t is time, p is pressure, and Re is the Reynolds number U_0H/ν (U_0 is the reference velocity at the step, H the reference height beyond the step and ν the kinematic viscosity of the fluid). All quantities in the above equations are non-dimensionalized using U_0, H and density ρ.

A convection conservative difference scheme based upon SOLA algorithm is used for the solution of the two-dimensional viscous incompressible unsteady Navier-Stokes equations

The central and partial donor convective difference scheme of conservation form satisfying the 2nd spatial accuracy on the regular grid in the original SOLA method[5] was revised on irregular staggered grids. The simple interior division principle in algebraic mathematics was adopted to correct irregular grid spacing to preserve the conservation forms as shown in Fig.1. Its artificial viscosity was reported from Hirt's stability analysis method[6]. The governing equations are given in terms of two-dimensional viscous incompressible unsteady flows.

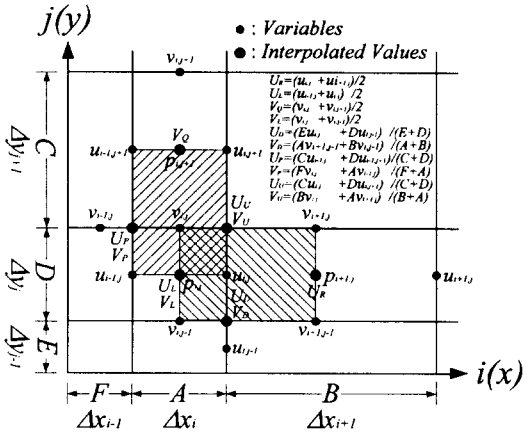

Fig. 1 Distribution of Physical Variables on Irregular Grid

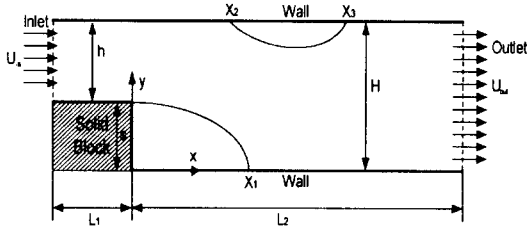

Fig. 2 Schematic of Calculation Domain

The viscous and pressure gradient terms are also corrected for irregular grid distribution to preserve the 2nd – order accuracy. The weighting factor, α, of partial donor terms is 0.2 for all the cases of computation. Time marching is explicitly Eulerian and the cycle convergence criterion is 0.002, maximum divergence at all grids. Dimensionless time(T) for data sampling interval is 1 and calculation is terminated at T=300.

Fig.2 is the schematic description of backward – facing step flow field in which two – dimensional poiseulle flow is adopted as laminar flow and it is assumed that steady velocity profiles which are average velocity 1 in the internal flow field and velocity 0 on the wall are selected for the transitional and turbulent flow. The twenty kinds of Reynolds number at

Table 1 Computational Conditions

Item		Computational Conditions		
Channel Height	H	1		
Step Height	s	0.49		
Reynolds Number	Re	10^2	1.5×10^2	3.0×10^2
		3.89×10^2	4.5×10^2	5.0×10^2
		6.0×10^2	6.5×10^2	7.0×10^2
		8.0×10^2	10^3	1.2×10^3
		2.0×10^3	3.0×10^3	4.0×10^3
		5.0×10^3	6.0×10^3	6.6×10^3
		7.0×10^3		1.76×10^5
Grid Number	MX×NY	250×40		
Maximum Grid Size	1/5H	0.2		
Minimum Grid Size	1/67H	0.015		
Boundary Condition	-	No Slip		
In Flow Condition	U_{in}	$U(y)=\frac{3}{2}V\left[1-\left(\frac{y}{a}\right)^2\right]$		
Out Flow Condition	U_{out}	$\frac{\partial U}{\partial x}=0, \frac{\partial v}{\partial x}=0, P=0$		
Finishing Time	T	300		

which the experimental data can be available for the backward-facing step are used for the calculations.

The no-slip condition is selected as the boundary condition to the walls. At the outlet of flow field, The Neumann condition is adopted for the velocity and The Dirichlet condition is used for the pressure. The above computational conditions are shown in Table 1 briefly.

In an effort to demonstrate that the reported solutions are dependent on the mesh refinement, computations are performed on seven different meshes of uniformly increasing refinement. Fig.3 shows dependence of reattachment length on the mesh number. However, though the mesh number of grid 46 ×46 is smaller than that of grid 250×20, the reattachment length result in contrary tendency. This fact means that the result of numerical calculation is influenced by the aspect ratio of grid size.

Also in order to investigate the result of inflow dependence, two kinds of the inflow profile are chosen for the laminar flow as shown in Table2. The selected two inflow profiles are both parabolic in shape but the result of calculation shows large difference of reattachment length.

An adopted grid distribution method is the algebraic and irregular grid system which shows that the grid size of step corner and walls are relatively more dense than that of inlet and outlet of the flow field in order to show flow phenomena in detail as shown in Fig.4. Irregular grid number is 250×40 and its minimum size is about 1/67 of the channel height(H) and its maximum is about 1/5H. The step height is 1/2.06H which was adopted to match the dimension with a experimental apparatus of Armaly et al..

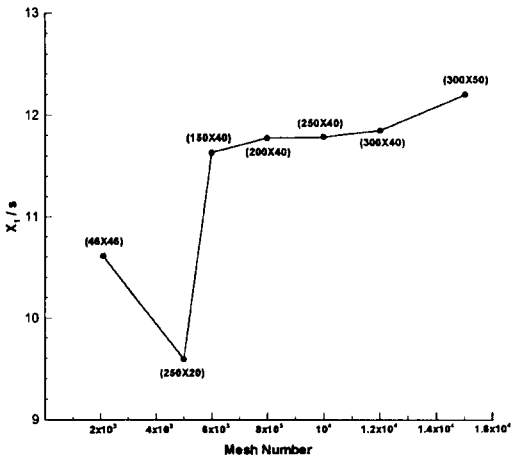

Fig.3 Grid Dependence of Reattachment Length

Table 2 Inflow Profile Dependence

Equation	$U(y)=\frac{3}{2}V\left[1-\left(\frac{y}{a}\right)^2\right]$	$U(y)=24y\left(\frac{H}{2}-y\right)$
Re	10^3	10^3
Grid size	250×40	250×40
X1/s	11.78	12.02

The one-dimensional stretching function which is an algebraic and irregular grid generation technique to minimize the errors on the satisfaction of the discretized continuity is used for distributing points irregularly along a particular boundary so that specific regions of the domain can be resolved accurately.

The stretching function is defined as follows:

$$s=P\eta^*+(1-P)\left(1-\frac{\tanh[Q(1-\eta^*)]}{\tanh Q}\right) \qquad (4)$$

where, an appropriate normalized independent variable would be

$$\eta^*=\frac{\eta-\eta_A}{\eta_E-\eta_A}$$

so that $\eta_A\le\eta\le\eta_E$ as $0\le\eta^*\le1$

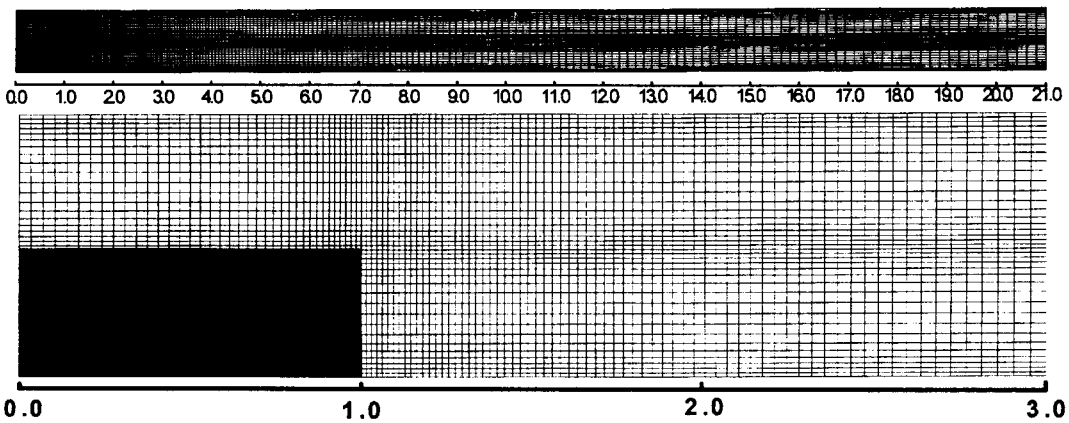

Fig. 4 Computational Grid

η_A and η_E are the start and end point. P and Q are parameters to provide grid point control. P effectively provides the slope of the distribution, $s \approx P\eta^*$, close to $\eta^* = 0$. Q is called a damping factor and controls the departure from the linear s versus η^* behavior. Typical distributions of points on EA, for various values of P and Q, are shown in Fig.5. The value of Q in this study is 2.0 which was determined by appropriate correction.

To determine the P value, two conditions are considered : 1) the first grid lengths from the step corner in the directions of the upstream and downstream region are equal ; 2) the grid density upstream and downstream from the step corner is interpolated easily.

The equation (5) is derived from the equation (4) to satisfy the conditions of selecting P value.

$$P = \frac{x - \tanh(Qterm)}{\frac{1}{n} - \tanh(Qterm)} \qquad (5)$$

and $Qterm$ is defined as,

$$Qterm = 1 \frac{\tanh[Q(1 - \frac{1}{n})]}{\tanh Q}$$

where x is the first grid length from the step corner and n is end point location.

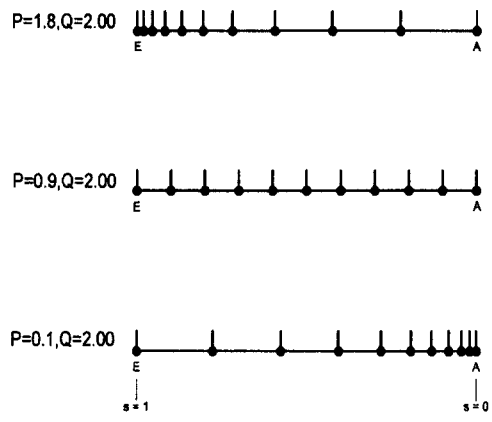

Fig. 5 Grid Distribution Using Equation(5)

3. RESULT AND DISCUSSION

The present study carried out calculations for twenty kinds of Reynolds number to examine the change of reattachment length downstream from backward step.

For the comparison of calculated results, available experimental data of Armaly et al. are used through laminar to turbulent flow region.

Fig.6 indicates comparison of experimental and theoretical results for the reattachment length up to $Re = 8.0 \times 10^2$ for the ten kinds of Reynolds number.

The numerical predictions presented in this paper confirmed that SOLA based computer code for flow predictions can be successfully employed to compute backward - facing step flows, with results in close agreement with experiments, at least up to the Reynolds number of approximately $Re = 4.0 \times 10^2$.

Fig.7 shows measurements of reattachment length of first recirculation region as a function of Reynolds number. According to the experimental result of Armaly et al[1], the laminar flow range is characterized by a reattachment

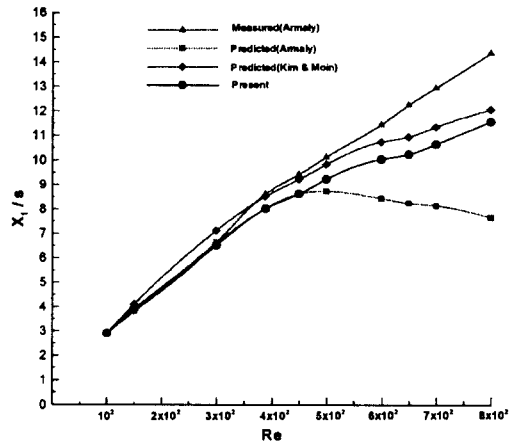

Fig. 6 Comparison of Experimental and Theoretical Flow Results

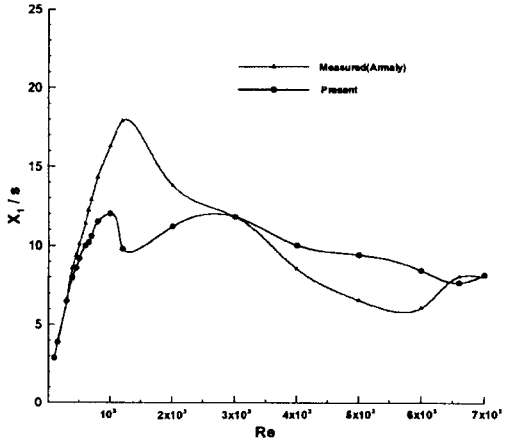

Fig. 7 Variation of Reattachment Locations with Reynolds Number

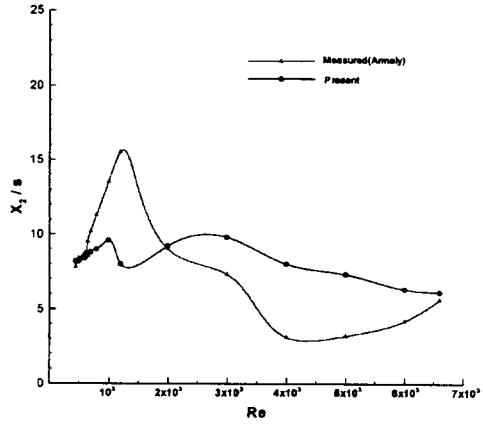

Fig. 8 Variation of Detachment Location with Reynolds Number

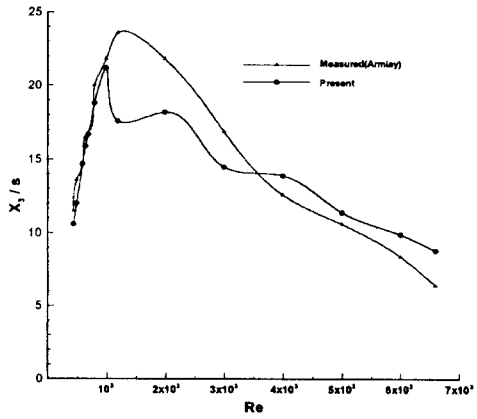

Fig. 9 Variation of Reattachment Locations with Reynolds Number

length that increases with Reynolds numbers up to $Re=1.2\times10^3$. From the part of first sharp decrease in the reattachment length x_1 to a minimum value at a Reynolds number of approximately 5.5×10^3, then an increase to a constant level, which are classified into transitional flow region. The turbulent flow range is characterized by a constant reattachment length at approximately above $Re=6.6\times10^3$.

However, present numerical results show a sharp decrease of reattachment - length from the $Re=1\times10^3$ and recovery of the length after $Re=1.2\times10^3$, then a meeting point at $Re=3\times10^3$. It is assumed that differences of reattachment length between the experimental and numerical results are attributed to the inlet velocity profile selected. A parabolic velocity profile which was used in this study for the laminar inlet velocity profile up to $Re=1\times10^3$ has good results of reattachment length in comparison with experimental results. But there are disagreement of reattachment length above $Re=1.2\times10^3$ to $Re=6.6\times10^3$, then the reattachment length is recovered nearly to the experimental result at the turbulent flow region.

Fig.8 and Fig.9 depict the lengths of separation points and reattachment points of secondary recirculation region at the upper wall and the numerical results are very close approximation to the available experimental data.

Fig.10 represents instantaneous flow characteristics which is generated beyond the backward - step at $Re=1\times10^3$.

Velocity vectors are shown in the entire flow field and five kinds of Dimensionless time(T= 5, 30, 100, 200 and 300) are selected to simulate instantaneous flow.

At T=5, there is the first recirculation region which is developing beyond the backward - step as well as a secondary recirculation region in the upper wall.

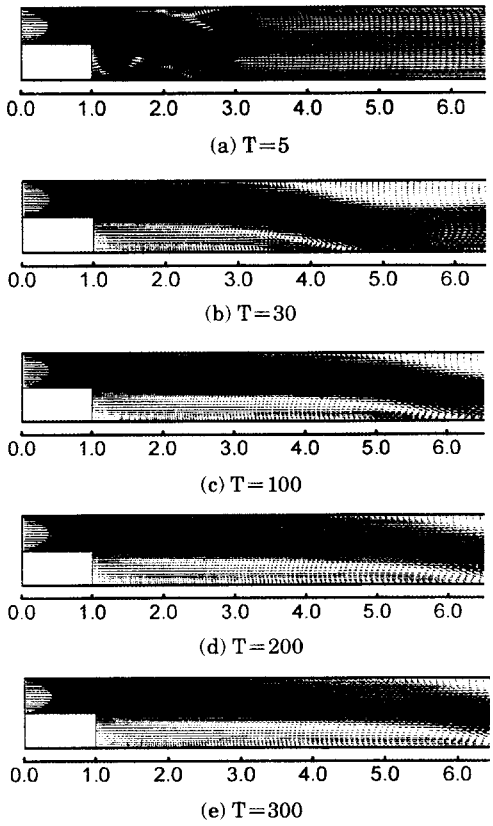

Fig. 10 Instantaneous Velocity Vectors ($Re=10^3$)

The secondary vortex in the first recirculation region gradually disappears and the reattachment length of the region becomes longer at T=30.

At T=100 and T=200, The two recirculation region in the bottom and upper wall are still developing and instantaneous velocity vectors downstream of the step are almost symmetric.

At T=300 the flow pattern of entire flow field and the reattachment length of first recirculation region are similar to Fig.10d(T=200). Therefore, it is assumed that the flow at T=300 is fully developed.

Fig.11 indicates time mean flow characteristics of velocity vectors, pressure distribution, vorticity contours, contours of u and v direction fluid speed and contours of kinetic energy at

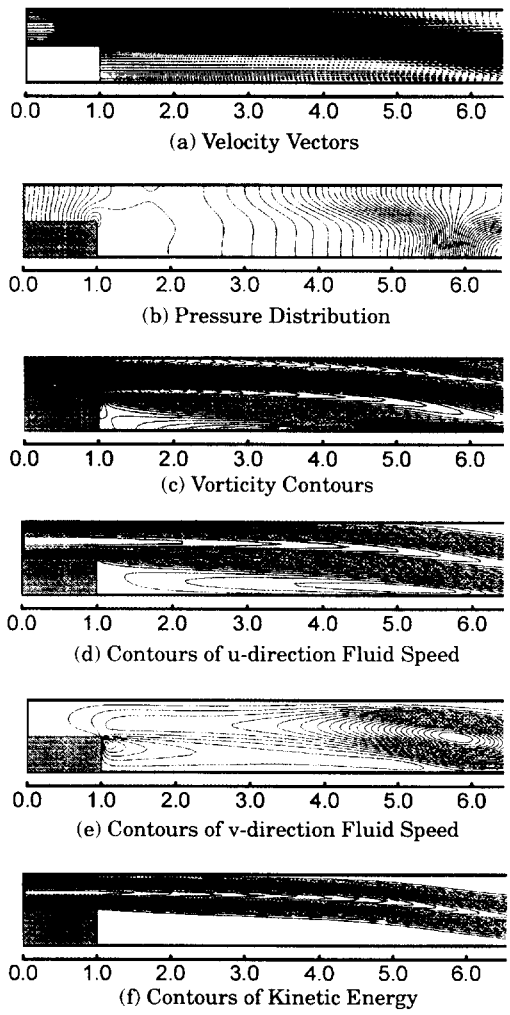

Fig. 11 Time-Mean Flow Characteristics at $Re=8\times10^2$ (T=200-300)

$Re=8\times10^2$ (T=200-300).

The inlet velocity profile is parabolic and the first and second recirculation regions are shown in Fig.11(a). Fig.11(b) and Fig.11(c) show the numerical results of pressure distribution and vorticity contours.

Fig.11(d) and Fig.11(e) depict the contours of u and v direction fluid speed, which shows the recirculation regions in the bottom and upper walls. The speed directions and high intensity area can be found easily. Contours of kinetic energy are uniform to the streamwise direction

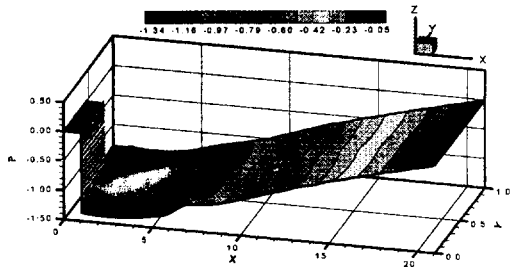

(a) Re=10^3

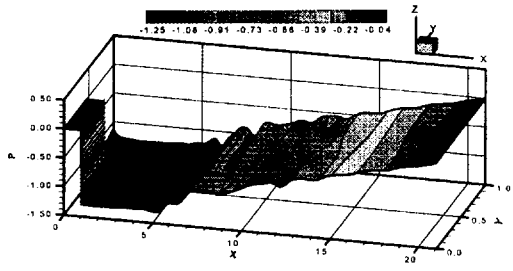

(b) Re=3×10^3

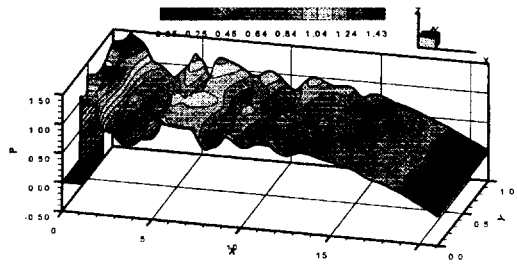

(c) Re=1.76×10^5

Fig. 12 Instantaneous Pressure Distribution (T=300)

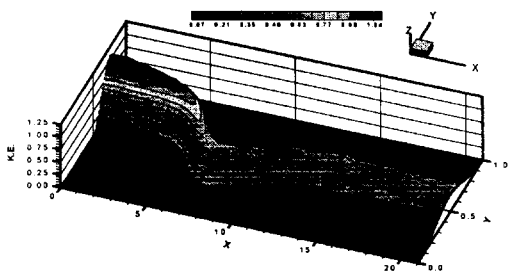

(a) Re=10^3

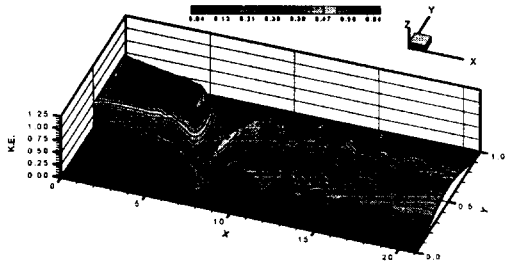

(b) Re=3×10^3

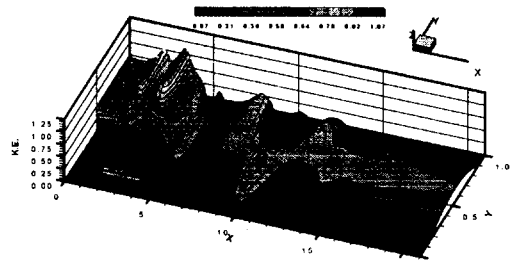

(c) Re=1.76×10^5

Fig. 13 Instantaneous Contours of Kinetic Energy (T=300)

as shown in Fig.11(f).

Fig.12 shows the instantaneous pressure distribution at dimensionless time T=300 for each Reynolds numbers. As Reynolds number is increased, the pressure fluctuation gets gradually higher.

The distribution of kinetic energy varies as Reynolds number is altered as shown in Fig.13. Also as Reynolds number is increased, we can see the appearance of a kinetic energy region behind the step corner in Fig.13(b) and Fig.13(c). Therefore, it is postulated that the distribution of kinetic energy is dependent on Reynolds number.

Fig.14 depicts time-mean flow characteristics of backward-facing step on each properties in the flow field at a relatively high Reynolds number Re=1.76×10^5. Pressure is graduallies recovered as flow runs to the downstream area as shown in Fig.14(a). And Fig.14(b) shows that high vorticity region is located around the step corner and the lowest part of vorticity is in the

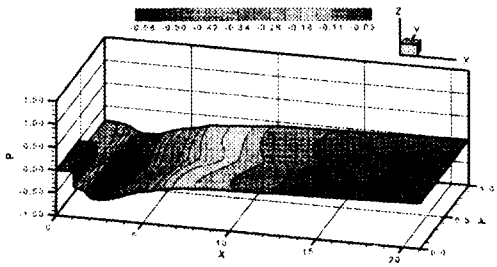

(a) Pressure Distribution

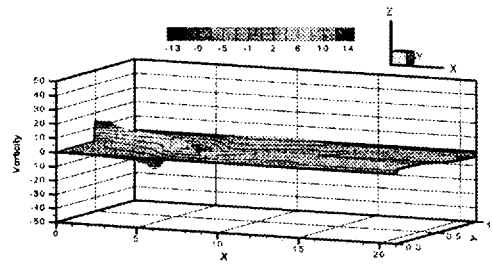

(b) Vorticity Contours

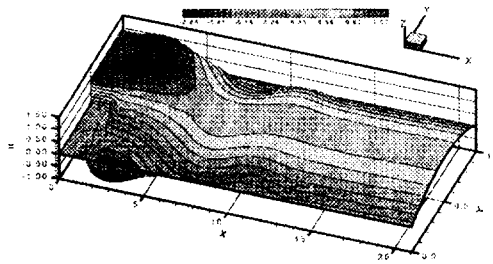

(c) Contours of u – direction Fluid Speed

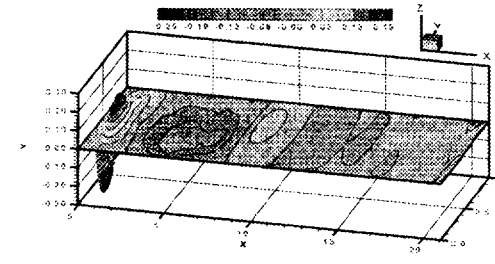

(d) Contours of v – direction Fluid Speed

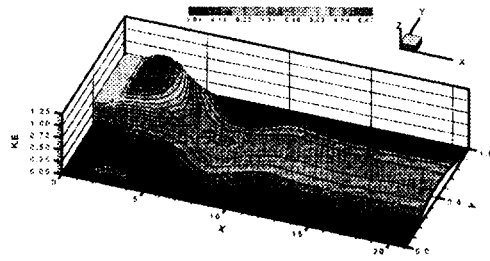

(e) Contours of Kinetic Energy

Fig. 14 Time – Mean Distribution ($Re = 1.76 \times 10^6$, T = 200 – 300)

center area of the upstream over the step. Fig.14(c) and Fig.14(d) indicate the distribution of fluid speed to the both streamwise and normal directions and also express the magnitude of fluid speed. The high kinetic energy area is the same as the high speed area.

4. CONCLUSION

Numerical calculations are carried out for the laminar, transitional and turbulent flows over a backward – facing step using a convection conservative difference scheme based upon SOLA algorithm and comparisons are made with available experimental results.

For the selected Reynolds numbers, the computation results obtained by the present methods show reasonably good agreement with the experimental data and especially the reattachment length is predicted in close agreement with the experimental values of the previous result. However, Some differences are found at the transitional region and more detailed studies are requested to have proper transitional inflow profile.

The flow over a backward facing step has not been fully understood yet because of its complex flow characteristics. So further computational and experimental studies are necessary to understand the flow phenomena.

REFERENCES

1. B.F.Armaly, F.Durst, J.C.F.Pereira and B.Schonung, "Experimental and Theoretical Investigation of Backward-Facing Step Flow", J. Fluid Mech., Vol.127, pp.473 - 496, 1983.
2. J.K.Eaton, J.P.Johnston, "A Review of Research on Subsonic Turbulent Flow Reattachment", AIAA J., Vol.19, No.9, pp.1093 - 1100, 1981.
3. J.Kim, S.J.Kline, J.P.Johnston,"Investigation of a Reattaching Turbulent Shear Layer: Flow Over a Backward-Facing Step", ASME J. Fluids Eng., Vol.103, pp.302 - 308, 1980.
4. KSME CFD Workshop on Backward-Step Flow Analysis, Thermo-Fluid Section, 1995.
5. C.E.Hirt, "Heuristic Stability Theory for Finite Difference Equations", J. Comp. Phys. Vol.2, pp.339 - 355,1968.
6. Y.H.Lee, J.G.Kim, D.W.Cho, "High Reynolds Number Flows within 2-Dimensional Lid-Driven Square Cavity", Proc. JSME Centennial Grand Congress, Int. Conf. on Fluid Eng., Vol.3, pp.1689 - 1694, 1997.

저 자 소 개

최영도(崔永都)
1970년 6월생. 1996년 한국해양대학교 이공대학 기계공학과 졸업, 1998년 한국해양대학교 대학원 기계공학과 졸업(석사), 1996~현재 대우중공업(주) 항공사업본부 사원. 당학회 회원.

이영호(李英浩)
1957년 2월생. 1980년 한국해양대학교 기관공학과 졸업, 1982년 한국해양대학교 대학원 석사과정 수료, 1989년 동경대학 기계공학과 박사과정 수료, 1980년~현재 한국해양대학교 조교, 전강, 조교수, 부교수(기계공학부), 당학회 편집위원('97, '98년도)